

Dynamic Exergy Analysis of an Solar-Assisted Ejector Cooling System

Fatih Akkurt

Department of Energy Systems Engineering, Faculty of Engineering and Architecture,
Necmettin Erbakan University, Konya, Turkey

ABSTRACT

In this paper, the exergy analysis of solar-assisted ejector cooling system (SAECS) was investigated for a day. Experiment was performed on the in July, from 09:00 to 17:00 in Konya, Turkey. The SAECS was the combination of two subsystems including solar cooling subsystem (SCS) and ejector cooling subsystem (ECS). Single-glazed selective-type collectors at a horizontal position were used. The collection area was 9.2 m². The ejector area ratio was 7.17. During the experiment evaporator temperature (T_e) was kept at 8 °C, while condenser temperature (T_c) was at a range of 26 and 28 °C. Exergy analysis was applied independently for each subsystem. The largest exergy destruction in ECS took place in the ejector followed by generator, condenser, and evaporator, respectively. Exergy efficiency of SCS was between 14 and 17 percent during the day and was increasing depending on the increase of the solar radiation. Exergy efficiency of ECS varied between 28.4 and 42.5 percent while exergy efficiency of SAECS varied between 4.5 and 6.4 percent depending on the solar radiation change during the day.

Keywords: Ejector cooling system, experimental, exergy analysis, maximum COP values

1. INTRODUCTION

Efficiency is one of the important factors for the systems that energy is consuming or producing because of the investment costs and the limit of resources. As, the renewable energy systems generally have lower efficiency than conventional systems, their efficiency becomes more important while utilizing them. Solar-assisted ejector cooling system is one of the cooling technologies that solar energy can be used, but it has a drawback of low COP value. Their COP values were obtained 0.3-0.8 while collector temperatures were between 80-150 °C Abdulateef et al [1]. In order to minimize this drawback, many researches focused on efficiency and system losses. Exergy analysis is one of the methods to understand the magnitude and reasons of these losses.

Alexis[2] studied about exergy loss and coefficient of performance of a steam-ejector refrigeration system. He determined that the most exergy destruction was at ejector and later condenser of the system. Arbel et al [3] stated that ejector irreversibility with including mixing, the kinetic energy losses and the normal shock wave. Sadeghi et al [4]. discovered that the generator has the highest exergy destruction followed by the ejector. Chen et al [5] determined that the ejector was responsible from the highest exergy destruction and later the generator and the condenser. Yan et al [6]. studied solar driven ejector compression heat pump cycle and they determined that the largest exergy destruction is generated in the ejector with an amount to 25.7% of the total system exergy input, followed by condenser and evaporator.

The purpose of this study was to investigate dynamic exergy analysis of an SAECS for a day. Variations in COP and cooling capacity of ECS and exergy input, exergy output and exergy destructions of both whole system were presented during solar exposure. The ejector area ratio was 7.17. The evaporator temperature was kept 8°C while condenser temperature was changing at a range of 26°C and 28°C. The experiment was performed at 0° tilt angle and 9.2 m² collector area.

2. SYSTEM DESCRIPTION

Experimental setup of SAECS was schematically shown in Fig.1. The system consists of combination of two subsystems. While using water in the heating cycle, R123 refrigerant was used in ejector cooling cycle. The ejector subsystem consists of a vapor generator, an ejector with movable nozzle, a condenser, a receiver tank, an expansion

valve, an evaporator, a sub-cooler and a sliding vane pump; on the other hand single-glazed and selective surface solar collectors are the devices of solar collector subsystem.

As the most important device of cooling system, ejector consists of a supersonic nozzle, a mixing chamber and a conical diffuser as shown in Fig.2. The operation of ejector cooling cycle is as follows: The primary vapor \dot{m}_p at the high pressure leaving the generator enters the supersonic nozzle. The very high velocity vapor at the exit of the nozzle produces a high vacuum at the inlet of mixing chamber and entrains secondary vapors into the chamber from the evaporator. The two streams first mix in the mixing chamber, and then, the pressure of the mixed stream rises to the condenser pressure in the diffuser. The mixed stream discharges from the ejector to the condenser. One part of the liquid refrigerant leaving the condenser enters the evaporator after passing through the expansion valve, and the other part flows to the liquid pump. The pump increases its pressure to the generator pressure.

A pyranometer was used to measure solar radiation. The pressures of the refrigerant were measured by pressure transmitters. The temperatures measured by Pt100 sensors. A heat meter was used to measure the flow rates $\dot{m}_{w,sc}$ and T_a and T_b temperatures of solar collector. The vaporization rate of the primary refrigerant \dot{m}_p at various generator temperatures in the nozzle was determined by measuring the time period of vaporization of a defined liquid refrigerant volume in the generator. Heat inputs \dot{Q}_{gen} and primary vapor flow rates \dot{m}_p , as a function of the generator temperature, were determined for throat diameter of 3.21 mm. Cooling water rate of condenser and chilling water rate of evaporator, $\dot{m}_{w,cond}$ and $\dot{m}_{w,eva}$, were measured by flow meters. After \dot{Q}_{eva} was determined and later the rate of the secondary refrigerant \dot{m}_e was calculated with heat transfer equation between refrigerant and chilling water. Pressures and temperatures were measured with an accuracy of ± 0.5 kPa and $\pm 0.5^\circ\text{C}$, respectively. The flow rates were measured with an accuracy of $\pm 0.1\%$ and the measurements of solar radiation and of heat input were determined with an accuracy of $\pm 2.5\%$ and $\pm 0.6\%$, respectively.

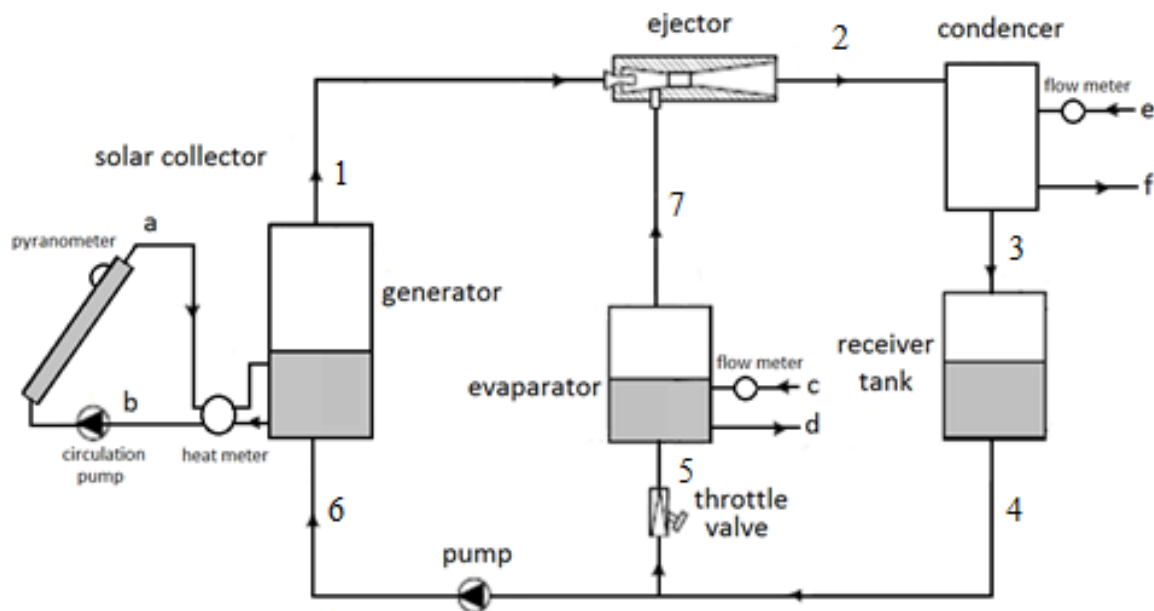


Figure 1: Solar-assisted ejector cooling system

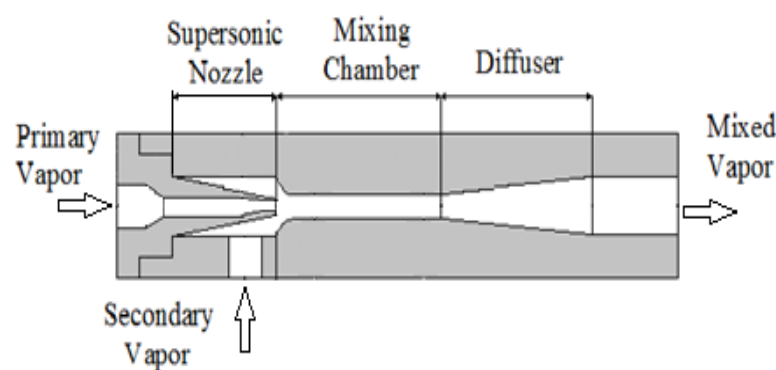


Figure 2: Ejector Model

COP of the ejector cooling system was calculated by using equation (1):

$$\text{COP} = \dot{Q}_{\text{eva}} / \dot{Q}_{\text{gen}} \quad (1)$$

\dot{Q}_{eva} and \dot{Q}_{gen} is the cooling capacity and heat input to the vapor generator and they were calculated by using equation (2) and equation (3), respectively. \dot{m}_s is the secondary vapor flow rate and \dot{m}_p is the primary flow rate. Specific enthalpies of the refrigerant at the inlet and outlet of the generator are h_5 and h_7 . $\dot{m}_{w,\text{eva}}$, T_c and T_d are flow rate and the temperatures of chilling water at the inlet and outlet of the evaporator.

$$\dot{Q}_{\text{eva}} = \dot{m}_{w,\text{eva}} c_p (T_c - T_d) \quad (2)$$

$$\dot{Q}_{\text{gen}} = \dot{m}_p (h_1 - h_6) \quad (3)$$

There is an optimum generator temperature for every area ratio where maximum COP can be obtained Yapici et al [7]. When the generator temperature reached to its optimum level, secondary vapor chokes at the inlet section of the mixing chamber and that causes the cooling capacity continue at a constant value. Variation in solar radiation and generator temperature were presented in Fig.3. It was determined that the optimum generator temperature and maximum COP value was determined 73.5°C and 37% for ejector area ratio of 7.17. The solar radiation values and generator temperatures were presented in Fig.4. The radiation value measured as 758 W/m² at 9 o'clock, it reached to a maximum value of 1081 W/m² in the middle of the day and was measured as 785 W/m² at 17 o'clock at the end of the experiment. The generator temperature initially was 66°C at the beginning of the experiment, reached to a maximum degree of 74.8°C in the middle of the day and later decreased to 66.9°C at the end of the experiment. As the optimum generator temperature was 73.5°C cooling system worked in choked conditions only between 12 and 15 o'clock.

Variation in cooling capacity and COP value during the experience were presented in Fig.5. At the beginning of the experiment cooling capacity and COP value were determined 296W and 15.8%, respectively. When ECS begun to work in choked condition at 73.5°C, the cooling capacity reached 926 W and the COP value was 37.3% as maximum values that system reached for ejector area ratio of 7.17. According to the increasing of generator temperature between 12 and 15 o'clock, cooling capacity remained approximately constant but the COP begun to decrease. At 15 o'clock the generator temperature reached to the optimum value, COP were the maximum again. Both cooling capacity and COP dropped to 368W and 19% end of the experience, respectively.

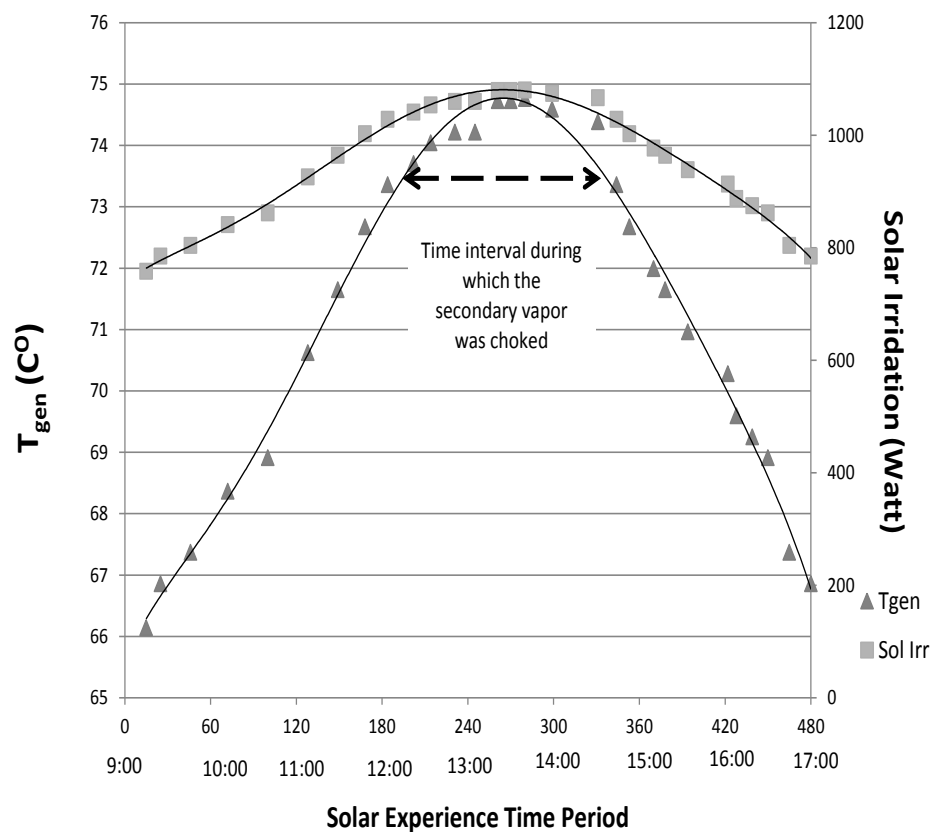


Figure 3: Variation in solar irradiation and generator temperature during the experience

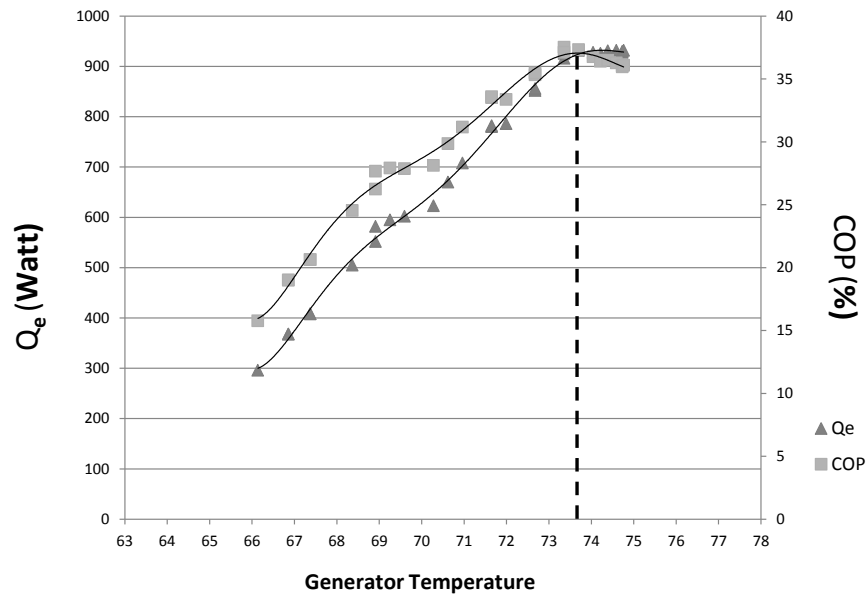


Figure 4: Variations in the cooling capacity and COP with generator temperature

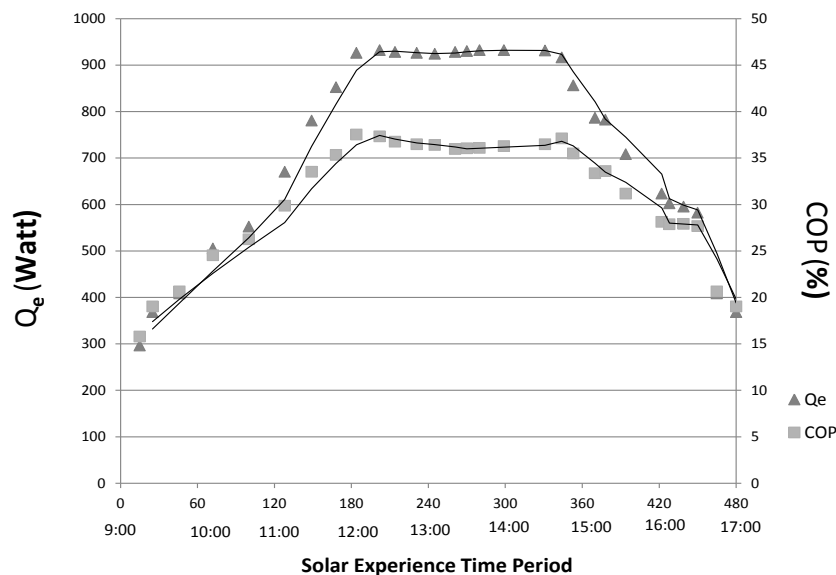


Figure 5: Variation in cooling capacity and COP during the experience

3. EXERGY ANALYSIS

Exergy analysis method is used to determine the maximum work potential of a system. This method better reveals the losses in the system than energy analysis. In this study exergy analysis method was carried out separately in two subsystems in order to determine losses of every device in the system within a day.

A. Exergy Analysis of Solar Collector Subsystem

Kotas[8], proposed some equations for exergy analysis. The equations which were used in exergy analysis for the collector subsystem were presented in Table 1.

In exergy analysis, environmental temperature T_o , varied between 23-28 °C during the day. T^* is approximately 3/4 of T_{sun} , which is black body temperature of the sun at about 5770 K. Heat transfer coefficient between the collector and the environment U_L , obtained 0.55 from the solar collector production company documentation. The solar collector temperature T_{sc} was taken as the average value of collector inlet and outlet temperature and varied between 71°C -84.3°C depending on the increase of solar radiation during the experiment.

Variation in exergy input, exergy output and exergy destruction rates of SCS during the experience were presented in Fig. 6. Curves of all three values during the experiment were similar, because the temperatures of the fluids entering and

leaving the solar collectors as well as the ambient temperature were similarly affected by solar radiation. Exergy input, destruction and output rates were calculated as 6551W, 5566W, 985W at the beginning of experiment, 9309W, 7711W, 1598W in the middle of the day, and 6777W, 5814W, 963W at the end of the experiment, respectively. A large proportion of exergy destructions were depending on the heat transfer in collector while a few of which were as a reason of heat loss from the collector to the ambient. The exergy destruction caused by heat transfer in collector can be explained with the transformation of solar radiation to heat on the solar collector and heat transfer from the solar collector to the working fluid. Majority of exergy destructions in collector was a reason of the temperature difference between the absorber plate surface and the sun Ge et al [9]. Another reason for the greatness of exergy destructions can be explained with the quality and type of solar collectors. Less exergy destructions can be obtained by using a better quality or other type solar collectors.

Table 1: Exergy equations used for SCS

Exergy balance for solar collector subsystem	$\dot{E}_{sc,in} + \dot{E}_{pump,cir} = \dot{E}_{sc,out} + I_{heat,trans} + I_{heat,loss}$
Energy balance of solar collector	$\dot{Q}_{sc,in} = \dot{Q} + \dot{Q}_o$
The energy flux coming from sun	$\dot{Q}_{sc,in} = \dot{q}^* A_{sc}$
The collector-ambient heat loss rate	$\dot{Q}_o = U_L A_{sc} (T_{sc} - T_o)$
Exergy input coming from solar radiation	$\dot{E}_{sc,in} = \dot{Q}_{sc,in} (1 - (T_o / T^*))$
Exergy destruction due to irreversible heat transfer	$I_{heat,trans} = \dot{Q} T_o (1/T_{sc} - 1/T^*)$
Exergy destruction due to irreversible heat loss between solar collector and ambient	$I_{heat,loss} = (\dot{Q}_{sc,in} - \dot{Q}) (1 - (T_o / T_{sc}))$
Exergy input coming from circulation pump	$\dot{E}_{pump,cir} = \dot{W}_{pump,cir}$

$\dot{E}_{sc,out}$: Exergy output of solar collector subsystem
 \dot{Q} : Heat transfer rate in solar collector
 \dot{q}^* : Solar radiation rate per meter square
 U_L : Overall heat transfer coefficient between the collector and the environment
 A_{sc} : Solar collector area
 T_o : Ambient temperature
 T^* : Temperature equal to $3/4 T_{sun}$
 T_{sun} : Black body temperature of the sun
 T_{sc} : Mean collector temperature
 $\dot{W}_{pump,cir}$: Energy consumption at the circulation pump

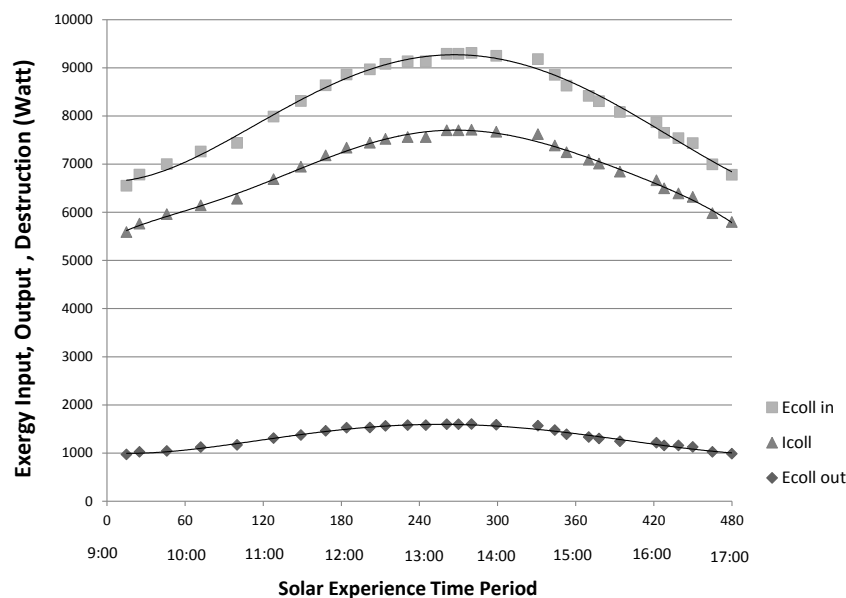


Figure 6: Variation in exergy input, exergy output and total exergy destruction of SCS during the experience

B. Exergy Analysis of ECS

Pridasawas and Lundqvist [10] proposed some equations for exergy analysis. The equations which were used in exergy analysis for ECS were presented in Table 2. It is important to know the exergy losses of the system for the efficiency of the system. By calculating the exergy destruction of each device in the system, the important devices that affect the system efficiency can be determined. Thus, relevant device can be focused to design and model the system. System efficiency can be increased by taking the necessary precautions to reduce exergy losses in the device.

Exergy destruction percentage of each device was calculated by using equation (4):

$$I_{\text{device}}(\%) = (I_{\text{device}} / \dot{E}_{\text{sc,out}}) * 100 \quad (4)$$

Variation in exergy destruction values and their percentages for ejector, generator, condenser and evaporator during the experience were presented in Fig.7 and 8. As it was seen in the figures, the maximum amount of exergy destruction was calculated in the ejector, both quantity and proportionally. Ejector irreversibility was the results of three main factors; mixing of primary and secondary refrigerants, the kinetic energy losses and the normal shock wave. The presence of these factors in the ejector is the main reason of the maximum exergy destruction among all the devices in ECS. The exergy destruction in the ejector is directly related to the refrigerant temperature coming from the generator and which increases with the increase of this temperature. Exergy destruction values and its percentages was calculated 329W and 34% at the beginning, 813W and 52% for the highest generator temperature and 365W and 37.2% at the end of the experiment. The exergy destruction curve in the ejector resembles the change curve of solar radiation during the day. It was seen that the most affected the device in terms of exergy destruction by generator temperature change was ejector compared to other devices in ECS. This is due to the complex physical events that take place in the ejector mentioned above. Improvements in design of the ejector geometry and optimization of working conditions will reduce the exergy destruction in the ejector.

Table 2: Exergy equations used for ECS

Exergy balance for ECS	$\dot{E}_{\text{sc,out}} + \dot{E}_{\text{eva}} + \dot{E}_{\text{pump}} = \dot{E}_{\text{cond,out}} + I_{\text{total}}$
The sum exergy destruction of all devices	$I_{\text{total}} = I_{\text{gen}} + I_{\text{cond}} + I_{\text{eva}} + I_{\text{eject}} + I_{\text{tv}} + I_{\text{pump}} + I_{\text{rt}}$
Exergy rate of evaporator	$\dot{E}_{\text{eva}} = \dot{Q}_{\text{eva}} (1 - (T_o / T_{\text{w,eva}}))$
Exergy rate of pump	$\dot{E}_{\text{pump}} = \dot{W}_{\text{pump}}$
Exergy destruction of generator	$I_{\text{gen}} = T_o (\dot{m}_p (s_1 - s_6) + \dot{m}_{\text{w,sc}} (s_b - s_a))$
Exergy destruction of condenser	$I_{\text{cond}} = T_o ((\dot{m}_p + \dot{m}_s) (s_3 - s_2) + \dot{m}_{\text{w,cond}} (s_f - s_e))$
Exergy destruction of evaporator	$I_{\text{eva}} = T_o (\dot{m}_s (s_7 - s_5) + \dot{m}_{\text{w,eva}} (s_d - s_c))$
Exergy destruction of ejector	$I_{\text{eject}} = T_o ((\dot{m}_p + \dot{m}_s) s_2 - \dot{m}_s s_7 - \dot{m}_p s_1)$
Exergy destruction of throttle valve	$I_{\text{tv}} = T_o (\dot{m}_s (s_5 - s_4))$
Exergy destruction of pump	$I_{\text{pump}} = \dot{W}_{\text{pump}} + \dot{m}_p ((h_6 - h_4) - T_o (s_6 - s_4))$
Exergy destruction of receiver tank	$I_{\text{rt}} = T_o ((\dot{m}_p + \dot{m}_s) (s_4 - s_3) + (\dot{Q}_{\text{rt}} / T_o))$
Heat transfer rate of receiver tank	$\dot{Q}_{\text{rt}} = ((\dot{m}_p + \dot{m}_s) (h_4 - h_3))$
$\dot{E}_{\text{sc,out}}$: Exergy input coming from solar collector \dot{E}_{eva} : Exergy inputs at the evaporator \dot{E}_{pump} : Exergy inputs at the pump $\dot{E}_{\text{cond,out}}$: Exergy output at the condenser \dot{Q}_{eva} : Cooling capacity of chilling water \dot{Q}_{rt} : Heat transfer rate in receiver tank $T_{\text{w,eva}}$: Cooling temperature of chilling water T_o : Ambient temperature \dot{W}_{pump} : Energy consumption at the pump $\dot{m}_{\text{w,sc}}$: Rate of water circulating in solar collector \dot{m}_p : Rate of primary refrigerant \dot{m}_s : Rate of secondary refrigerant $\dot{m}_{\text{w,cond}}$: Rate of cooling water $\dot{m}_{\text{w,eva}}$: Rate of chilling water h : Enthalpy at the specified point in the cycle s : Entropy at the specified point of the cycle	

The second biggest exergy destruction in ECS occurred in the generator and condenser at different times of experiment time period. As it was seen in the figure, exergy destruction values were less in the generator than condenser, due to the low generator temperature at the beginning of the experiment. Exergy destruction its percentages in the generator was calculated as 55W and 5.7% at the beginning of experiment. The increase in generator temperature due to the increase of solar radiation caused the exergy destruction in the generator rise to 140W and 9.1%, exceeding the exergy destruction in the condenser. At the end of the experiment, the exergy destruction values were reduced to 365W and 37.2%. Exergy destruction change was almost constant in the condenser throughout the experiment. However, due to the increase in the temperature of the cooling water in the middle of the day, exergy destruction decreased a bit. The average exergy destruction values in condenser were determined 122W and 9.7% throughout the day. Exergy destruction in the evaporator was also almost constant, because the temperatures of the refrigerant and cooling water entering and leaving the evaporator were approximately the same throughout the experiment. The average exergy destruction values in the evaporator were calculated as 56W and 4.1% throughout the experiment. Exergy destruction values in other devices of ECS were negligible when they were compared to devices above mentioned.

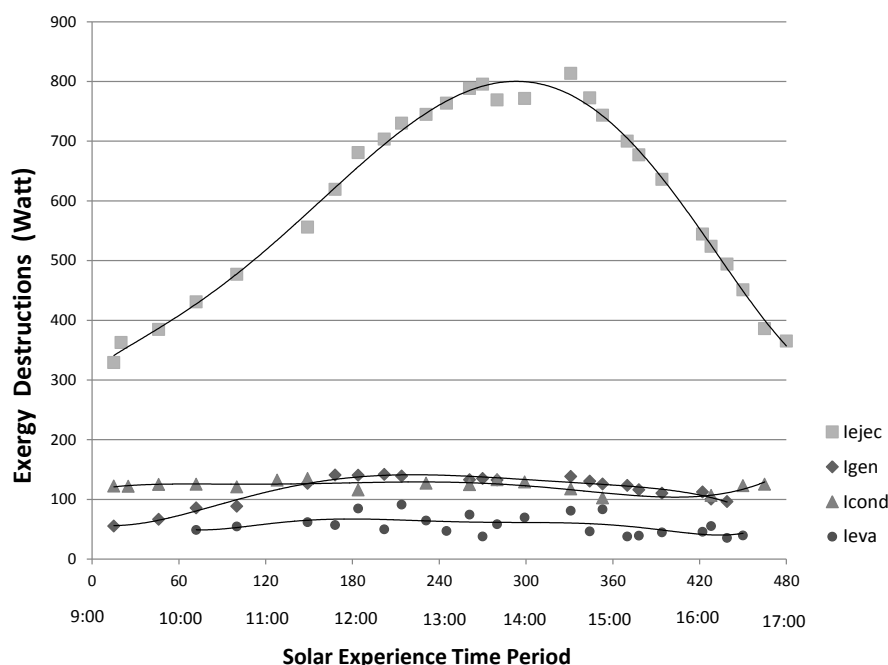


Figure 7: Variation in exergy destructions of ejector, generator and condenser during the experience

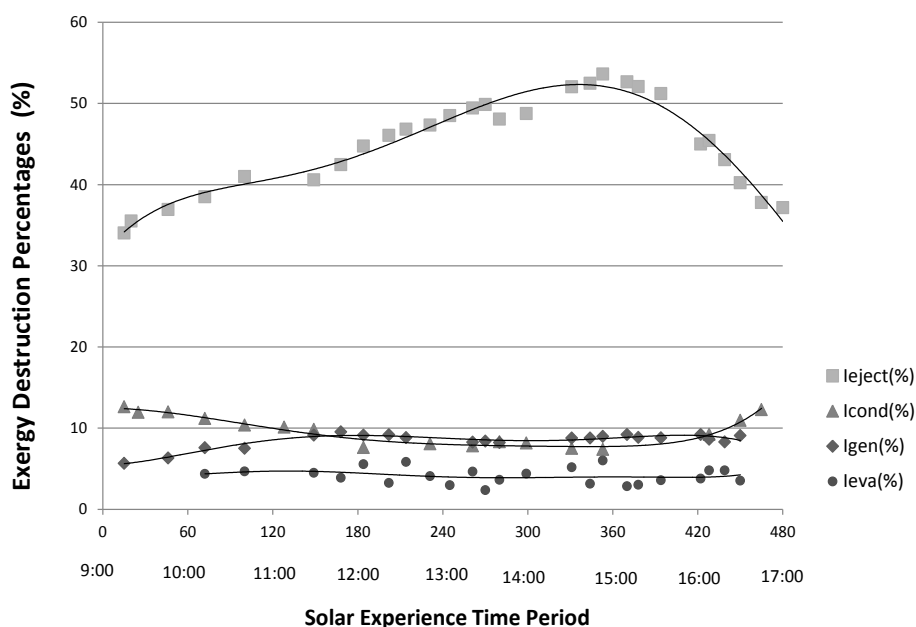


Figure 8: Variation in exergy destruction percentages of ejector, generator and condenser during the experience

Variation in exergy input, exergy output and total exergy destruction rates of ECS during the experience were presented in Fig. 9. The figure shows that total exergy destruction curve of ECS is similar to the exergy curve that enters to the system. Exergy input, destruction and output rates were calculated as 1033W, 1590W, 1030W at the beginning, 412W, 500W, 424W in the middle of the day, and 621W, 1090W, 606W at the end of the experiment, respectively. The main reason for the change in exergy input is the change in the solar radiation, but the predominant factor in the change of the exergy destruction in ECS can be expressed as exergy destructions in the ejector and generator depending on the temperature increases. Taking precautions to reduce the exergy destruction of these two devices will increase the efficiency of the cooling system. This can be done with the good design and optimization of working conditions of both devices.

Exergy efficiency of SCS ϵ_{SCS} , ECS ϵ_{ECS} , and total exergy efficiency of SAECS ϵ_{SAECS} , was calculated by using equation (5, 6 and 7):

$$\epsilon_{SC} = (\dot{E}_{sc,out} / \dot{E}_{sc,in}) * 100 \quad (5)$$

$$\epsilon_{ECS} = (\dot{E}_{cond,out} / \dot{E}_{sc,in}) * 100 \quad (6)$$

$$\epsilon_{SAECS} = (\dot{E}_{cond,out} / \dot{E}_{sc,in}) * 100 \quad (7)$$

According to the equation above exergy efficiency of collectors was calculated between 14 and 17 percent during the day and it was increasing depending on the increase of the solar radiation. Variation in total exergy efficiency values of SAECS during the experience were presented in Fig. 10. The figure shows that Exergy efficiency of ECS varied between 28.4 and 42.5 percent depending on the solar radiation change during the day. Exergy efficiency of SAECS varied between 4.5 and 6.4 percent depending on the solar radiation change during the day.

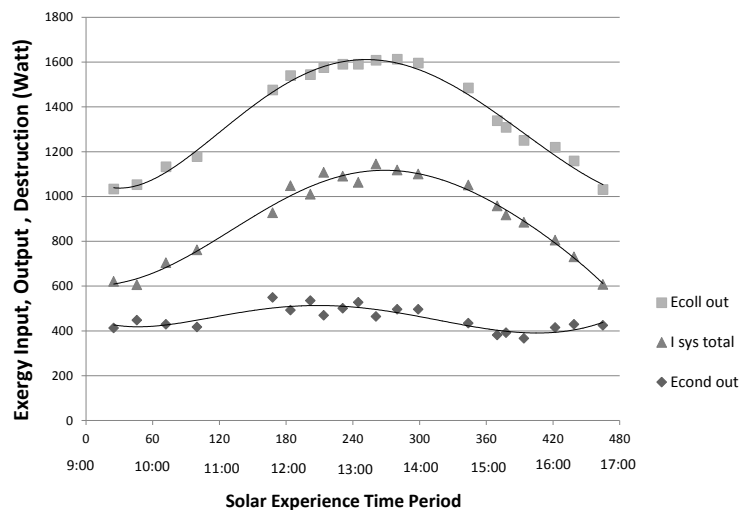


Figure 9: Variation in exergy input, exergy output and total exergy destructions of ECS during the experience

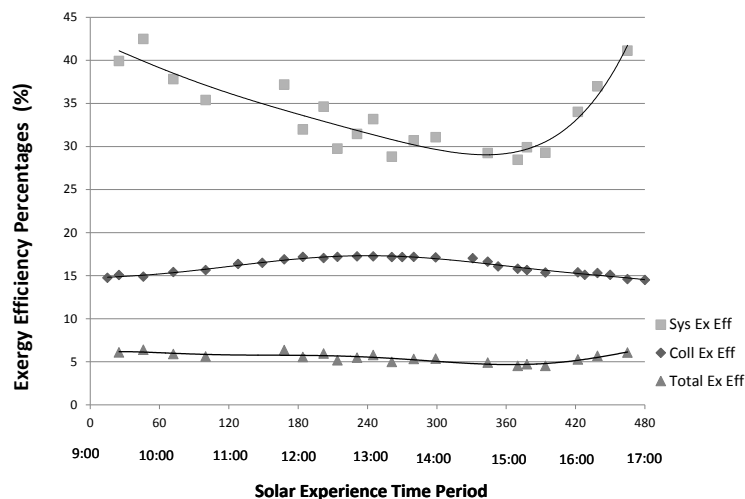


Figure 10: Variation in total exergy efficiency values of SAECS during the experience

CONCLUSION

In this study, exergy analysis of SAECS was investigated for a day. SAECS was the combination of two subsystems including SCS and ECS. Exergy destruction values are calculated for both subsystems. The quantity and proportion of exergy destruction were calculated for both subsystems. Exergy efficiency of collectors was between 14 and 17 percent during the day and was increasing depending on the increase of the solar radiation. A large proportion of exergy destructions in collector was depending on the heat transfer in collector while a few of which were as a reason of heat loss from the collector to the ambient. The maximum amount of exergy destruction was calculated in the ejector, both quantity and proportionally, as the reasons of mixing of primary and secondary refrigerants, the kinetic energy losses and the normal shock wave. Ejector geometry and optimization of working conditions will reduce the exergy destruction in the ejector. The exergy destruction of generator, condenser, and evaporator followed ejector, respectively. Exergy efficiency of ECS varied between 28.4 and 42.5 percent. Exergy efficiency of SAECS varied between 4.5 and 6.4 percent during the day depending on the effect of both subsystems.

REFERENCES

- [1]. J.M. Abdulateef, K. Sopian, M.A. Alghoul and M.Y. Sulaiman, "Review on Solar-Driven Ejector Refrigeration Technologies," *Renewable Sustainable Energy Reviews*, pp. 1338–1349, 2009.
- [2]. G.K. Alexis, "Exergy Analysis of Ejector-Refrigeration Cycle Using Water As Working Fluid," *International Journal of Energy Research*, pp. 95–105, 2005.
- [3]. A. Arbel, A. Shklyar, D. Hershgal, M. Barak and M. Sokolov, "Ejector Irreversibility Characteristics," *Journal of Fluids Engineering*, pp. 121–129, 2003.
- [4]. M. Sadeghi, S.M.S. Mahmoudi and R.K. Saray, "Exergoeconomic Analysis and Multi-Objective Optimization of an Ejector Refrigeration Cycle Powered by an Internal Combustion (HCCI) Engine," *Energy Conversion and Management*, pp. 403–417, 2015.
- [5]. J. Chen, H. Havtun and B. Palm, "Conventional and Advanced Exergy Analysis of an Ejector Refrigeration System," *Applied Energy*, pp. 139–151, 2015.
- [6]. G. Yan, T. Bai and J. Yu., "Energy and Exergy Efficiency Analysis of Solar Driven Ejector–Compressor Heat Pump Cycle," *Solar Energy*, pp. 243–255, 2016.
- [7]. R. Yapiıcı and C.C. Yetişen, "Experimental Study on Ejector Refrigeration System Powered by Low Grade Heat," *Energy Conversion and Management*, pp. 1560–1568, 2007.
- [8]. T.J. Kotas, "The Exergy Method of Thermal Plant Analysis," Butterworths, UK, 1985.
- [9]. Z. Ge, H. Wang, H. Wang, S. Zhang and X. Guan, "Exergy Analysis of Flat Plate Solar Collectors," *Entropy*, pp. 2549–2567, 2014.
- [10]. W. Pridasawas and P. Lundqvist, "An Exergy Analysis of a Solar-Driven Ejector Refrigeration System," *Solar Energy*, pp. 369–379, 2004.